IJMS
Vol 51, No 6, June 2026

Original Article

Surface-Engineered Selenium Nanoparticles with L-Asparagine and Tartaric Acid: Therapeutic Efficacy Against Breast Cancer and Bacterial Infections

Abdolrazagh Marzban[1#], PhD; Khadije Salari Nejad[2#], MD; Maryam Zand[3], PhD; Masumeh Jalalvand[2], PhD; Hamed Esmaeil Lashgarian[4], PhD

[1]Razi Herbal Medicines Research Center, Lorestan University of Medical Sciences, Khorramabad, Iran;
[2]Department of Medical Biotechnology, School of Medicine, Lorestan University of Medical Sciences, Khorramabad, Iran;
[3]Department of Medical Biotechnology, Zanjan University of Medical Sciences, Zanjan, Iran;
[4]Department of Medical Genetics and Biotechnology, School of Medicine, Lorestan University of Medical Sciences, Khorramabad, Iran
[#]The authors contributed equally to this work.

Correspondence:
Hamed Esmaeil Lashgarian, PhD;
Department of Medical Genetics and Biotechnology, School of Medicine, Lorestan University of Medical Sciences, Moalem St., Shahid Anoushirvan Rezaei Sq., Postal code: 6814933118, Khorramabad, Iran
Tel: +98 66 33300661
Email: Hamedlashkarian2@gmail.com
Received: 24 September 2025
Revised: 09 December 2025
Accepted: 28 December 2025

What's Known

- Selenium nanoparticles (SeNPs) possess strong antioxidant and anticancer properties with lower toxicity than other selenium forms.
- However, their biomedical application is limited by instability and aggregation in aqueous media, necessitating surface functionalization strategies to improve solubility, stability, and biological performance.

What's New

- Functionalization with tartaric acid and L-asparagine produced stable SeNPs with potent activity against antibiotic-resistant bacteria (MIC=0.071 mg/mL) and selective cytotoxicity toward breast cancer cells (IC_{50}=3.47 µg/mL), retaining efficacy at acidic pH.

Abstract

Background: Selenium nanoparticles (SeNPs), compared to other forms of selenium, have shown promising antioxidant and anticancer properties with lower toxicity. However, SeNPs precipitate and aggregate in aqueous solutions due to their high surface energy. To overcome this limitation and improve stability, solubility, and enhance biological efficacy, we functionalized them with L-asparagine/tartaric acid (Asn-Tar). This study aimed to evaluate the antimicrobial, cytotoxic, and antioxidant properties of SeNPs conjugated to Asn-Tar on MDA-MB-231 breast cancer cells.

Methods: This study was conducted at Lorestan, Iran, in 2023. SeNPs were synthesized using a co-precipitation method and then coated with Asn-Tar. Structural characterization was performed using Fourier transform infrared spectroscopy (FTIR), X-ray Diffraction (XRD), Scanning electron microscopy (SEM), Transmission electron microscopy (TEM), Dynamic light scattering (DLS), zeta potential analysis, and Ultraviolet-visible (UV-Vis) spectroscopy. Antioxidant activity was assessed. For biological evaluation, an *in vitro* experimental design was employed. Cytotoxicity against MDA-MB-231 breast cancer cells and normal fibroblast cells at various pH levels was determined using the 3-(4,5-dimethylthiazol-2-yl)-2,5-diphenyltetrazolium bromide (MTT) assay with three independent replicates per concentration (n=3). Antimicrobial activity against a panel of Gram-positive and Gram-negative bacteria, including antibiotic-resistant strains, was evaluated in triplicate using broth microdilution and well diffusion methods. Quantitative data are presented as mean±SD. Statistical significance was determined using Student's *t* test and one-way ANOVA, with $P<0.05$ considered significant.

Results: The synthesized Asn-Tar/SeNPs nanocomposite exhibited a spherical morphology with an average size of 460.8 nm, a negative zeta potential (-9.37±0.44 mV), and successful coating was confirmed by FTIR and XRD. The nanocomposite demonstrated dose-dependent antioxidant activity, with an IC_{50} of 22.73±1.55 µg/mL in the DPPH assay. It exhibited potent and selective cytotoxicity against MDA-MB-231 breast cancer cells (IC_{50}=3.47±0.28 µg/mL) compared to normal fibroblast cells (IC_{50}=5.91±0.34 µg/mL; P=0.0051). The nanocomposite retained approximately 50% of its cytotoxic activity at acidic pH (4.5). Furthermore, it showed strong antimicrobial activity, with inhibition zones up to 36.9±1.2 mm against *Staphylococcus saprophyticus* and MIC values as low as 0.035 mg/mL against *Pseudomonas aeruginosa*.

Conclusion: The produced Asn-Tar/SeNPs nanocomposite exhibited potent antimicrobial, selective cytotoxicity, and antioxidant properties. Our findings confirm the potential of these Asn-Tar/SeNPs nanocomposites for targeted therapy of breast cancer.

Please cite this article as: Marzban A, Salari Nejad K, Zand M, Jalalvand M, Esmaeil Lashgarian H. Surface-Engineered Selenium Nanoparticles with L-Asparagine and Tartaric Acid: Therapeutic Efficacy Against Breast Cancer and Bacterial Infections. Iran J Med Sci. 2026;51(6):403-416. doi: 10.30476/ijms.2026.108826.4394.

Keywords ● Selenium ● Breast neoplasms ● Nanoparticles ● Antioxidants

Introduction

Cancer is a complex disease, and its treatment faces many challenges. Conventional cancer treatments include chemotherapy and radiotherapy, which require new therapeutic tools and techniques due to their severe side effects.[1]

Today, nanotechnology has reduced systemic toxicity in cancer through targeted drug delivery systems and has created a major revolution in cancer treatment.[2] Nanoparticles (NPs) have emerged as practical tools in cancer therapy, with minimal side effects. Their efficacy is attributed to various mechanisms, including modulation of the tumor microenvironment and synergistic effects with existing therapies.[3] Nanoparticles have attracted much attention due to their nanometric size, large contact surface area, charge distribution, and their potential application in various ways. Nanoparticles with higher permeability allow for better delivery of hydrophilic agents and ionized drugs.[4]

Among metal nanoparticles, SeNPs have attracted much attention due to their unique properties. SeNPs have shown greater anticancer efficacy than inorganic or organic selenium compounds. They also have better stability, cellular uptake, and therapeutic efficacy with less systemic toxicity, and have been used to prevent cancer.[5, 6]

Selenium is an essential micronutrient that incorporates into antioxidant enzymes such as glutathione peroxidase and thioredoxin reductase, which play essential roles in regulating oxidative stress and cellular redox homeostasis.[7, 8]

Despite their properties, uncoated SeNPs often precipitate and aggregate in aqueous solutions, due to their high surface energy, limiting their biological activity. To overcome this limitation, SeNPs can be modified by functionalizing them with organic molecules such as amino acids, polysaccharides, folic acid (FA), hyaluronic acid, and others, which improves the stability and solubility of SeNPs. Furthermore, while SeNPs can accumulate in tumors due to their enhanced permeability and retention (EPR) properties, the uptake efficiency is approximately 1% or lower. The conjugation of SeNPs with ligands facilitates increased internalization of nanoparticles via receptor-mediated endocytosis and directs them to specific locations, thereby enhancing their targeted delivery and biological activity.[6, 9]

Amino acids serve as the fundamental components of proteins, comprising amine (–NH2), carboxyl (–COOH) functional groups, and distinct side chains in their structures. L-Asparagine possesses amine (–NH2), ammonium (NH3), methylene (CH2), and carboxyl (–COOH) functional groups.[10] Therefore, L-asparagine can bind to SeNPs, preventing selenium aggregation. Tartaric acid is a natural dicarboxylic acid known for its stabilizing, antioxidant, and potential targeting properties [11, 12] Coating SeNPs with these ligands (tartaric acid and L-Asparagine) can produce Asn-Tar/SeNPs nanocomposite with improved dispersion, reduced aggregation, and enhanced biological efficacy.

Therefore, this study aimed to synthesize L-asparagine and tartaric acid-functionalized selenium nanoparticles (Asn-Tar/SeNPs) and to assess their antimicrobial, antioxidant, and cytotoxic activities against the MDA-MB-231 breast cancer cell line.

Materials and Methods

Experimental Design

This *in vitro* experimental study was structured to synthesize, characterize, and evaluate the biological properties of L-asparagine and tartaric acid-functionalized selenium nanoparticles (Asn-Tar/SeNPs). This study was approved by the Ethics Committee of Lorestan University of Medical Sciences, Iran (IR.LUMS.REC.1400.294). The design encompassed three sequential phases:

Synthesis and Physicochemical Characterization

SeNPs were synthesized via a co-precipitation method and functionalized with L-asparagine and tartaric acid. The successful synthesis and key properties (size, morphology, charge, crystallinity, and functional groups) were confirmed using UV-Vis spectroscopy, Fourier transform infrared spectroscopy (FTIR), X-ray Diffraction (XRD), Scanning electron microscopy (SEM), Transmission electron microscopy (TEM), Dynamic light scattering (DLS), and zeta potential analysis.

Biological Activity Evaluation: The nanocomposite was evaluated for antioxidant capacity using DPPH radical-scavenging and H_2O_2-inhibition assays, with ascorbic acid as a positive control.

Cytotoxicity and selectivity against the human breast cancer cell line MDA-MB-231 versus normal fibroblast cells were evaluated using the MTT assay. Cells were treated with a concentration range of the nanocomposite (31.25–1000 µg/mL). Untreated cells served as the negative control. The stability of cytotoxic activity under acidic (pH ~4.5) and alkaline (pH ~8.5) conditions was also assessed.

Antimicrobial activity against a panel of Gram-positive and Gram-negative bacteria (including antibiotic-resistant strains) was tested using the well diffusion assay and the broth microdilution method to determine the Minimum Inhibitory Concentration (MIC) and Minimum Bactericidal Concentration (MBC). Chloramphenicol was used as a reference antibiotic (positive control).

Chemicals, Microbial, and Cell strains

Sodium selenite (Na2O3Se), tartaric acid, and L-asparagine were procured from Merck Chemical Company (Merck, Germany). All reagents, such as Diphenylpicrylhydrazyl (DPPH), (3-(4, 5-dimethylthiazol-2-yl)-2,5-diphenyl tetrazolium bromide (MTT), crystal violet, and Triphenyl tetrazolium chloride (TTC), were purchased from Sigma-Aldrich (Sigma-Aldrich, USA). All bacterial and fungal media cultures were from Quelab products, extra pure grade (Quelab, Canada). High-glucose Dulbecco's modified Eagle medium (DMEM) medium, penicillin-streptomycin, and fetal bovine serum (FBS) were obtained from Kiazist (Hamedan, Iran). Bacterial and fungal strains were procured from the microbial collection of the Iranian Research Organization for Science and Technology (IROST). MDA-MB-231 human breast cancer cell line was prepared from a cell collection of the Pasteur Institute of Iran (Tehran, Iran).

Biosynthesis

This study was conducted from 2022 to 2023 at Lorestan University of Medical Sciences, Khorramabad, Iran. Asn-Tar/SeNPs were synthesized via the co-precipitation method. Sodium selenite (Na_2SeO_3) was used as the selenium source, and tartaric acid and L-asparagine were used to functionalize the nanoparticles. One M solutions of each compound were prepared in 50 mL of sterile deionized water and dissolved using a magnetic stirrer. The solutions were then combined and incubated at room temperature for 24 h. The resulting mixture was centrifuged at 10,000 rpm for 15 min, and the precipitate was washed twice with deionized water and centrifuged again. The final pellet was freeze-dried to obtain the Asn-Tar/SeNPs nanocomposite.

Characterization

The composition, morphology, and physicochemical properties of Asn-Tar/SeNPs were characterized using ultraviolet–visible (UV–visible) spectrophotometry (Jenway 6505, UK), Fourier transform infrared spectroscopy (FTIR) spectroscopy (Bruker Tensor 27, Germany), emission scanning electron microscopy (FESEM) and energy dispersive X-ray (EDX) analysis (TESCAN MIRA3, Czech Republic), X-ray diffraction (XRD) (Bruker D8 Advance, Germany), and Transmission electron microscopy (TEM, Philips CM120, Netherlands). Particle size and phase analysis were performed using ImageJ (NIH, USA) and XPert-HighScore Plus 2.2 (Malvern Panalytical, The Netherlands) software.

Antimicrobial Assay

The antimicrobial activity of Asn-Tar/SeNPs nanocomposites was evaluated against both Gram-negative (*Klebsiella pneumoniae*, antibiotic-resistant *K. pneumoniae*, *Escherichia coli*, *Pseudomonas aeruginosa*, antibiotic-resistant *P. aeruginosa*) and Gram-positive (*Staphylococcus saprophyticus*, *Staphylococcus aureus*, *Bacillus cereus*) bacteria.

Well Diffusion Assay

Chloramphenicol solution (Sigma-Aldrich, USA) was used as a positive control. Fresh bacterial cultures (0.5 McFarland standard, 1×10^8 CFU/mL) were prepared in phosphate buffer. Four wells were made in agar plates, and each was inoculated with 0.5 McFarland bacterial suspension using a sterile swab. Subsequently, 20 µL of various concentrations of the nanocomposite (2.5, 5, 10, or 20 mg/mL) and antibiotic solution were added to the wells. Plates were incubated at 37 °C for 24 hours, and the diameters of inhibition zones were measured in millimeters (mm).

Minimum Inhibitory Concentration (MIC) and Minimum Bactericidal Concentration (MBC) Evaluations

The MIC was determined using the microbroth dilution method according to Clinical and Laboratory Standards Institute (CLSI) guidelines.[13] Briefly, 100 µL of Mueller-Hinton broth (Merck, Germany) was dispensed into each well of a microplate. Serial dilutions of Asn-Tar/SeNPs nanocomposite and chloramphenicol (Sigma-Aldrich, USA) were prepared, and 0.5 McFarland bacterial suspensions (1×10^8 CFU/mL) were added to each well. Plates were incubated at 37 °C for 24 hours. After incubation, 10 µL of TTC dye (Sigma-Aldrich, USA) was added to each well and incubated for an additional 3 hours to visualize microbial growth. Absorbance was measured at 600 nm using a spectrophotometer (BioTek, USA). Wells showing no visible growth after 24 hours were used to determine the MBC.

Effect of pH on Cytotoxicity

To evaluate the effect of pH on the biological properties of Asn-Tar/SeNPs, samples were incubated at either acidic (pH 4.5–5.0) or alkaline (pH 8.0–8.5) conditions for 1 hour at 37 °C, with pH adjusted using 1 N HCl or 1 N NaOH. The pH was then neutralized to 7.4, and cytotoxicity was assessed.

Antioxidant Assay

Antioxidant activity was evaluated using the DPPH radical scavenging assay. DPPH solution (0.1 mM in methanol; Sigma-Aldrich, USA) served as the oxidant, and ascorbic acid (Sigma-Aldrich, USA) was used as a positive control. One mL of DPPH solution was added to 4 mL of each sample (in 40% methanol) at concentrations of 0.78–50 µg/mL. After vortexing, samples were incubated in the dark at room temperature for 15 min. Absorbance was measured at 520 nm using a spectrophotometer (Jenway 6505, UK). Antioxidant activity was calculated as $(A_0-A_1)/A_0\times100$, where A_0 is the absorbance of the control, and A_1 is the absorbance with the sample.

Hydrogen Peroxide (H2O2) Inhibition Assay

Antioxidant activity was further assessed by hydrogen peroxide (H_2O_2) scavenging assay. Phosphate-buffered saline (PBS; Gibco, USA) was used as the blank, and ascorbic acid as the positive control. Samples at various concentrations (0.78–50 µg/mL) were mixed with H_2O_2 solution (35% w/w in deionized water; Merck, Germany) and incubated for 15 min with shaking. Absorbance was measured at 230 nm using a spectrophotometer (Jenway 6505, UK). Antioxidant activity was calculated as $(A_0-A_1)/A_0\times100$, where A_0 is the absorbance of the control, and A_1 is the absorbance of the sample.

Cytotoxicity Assay

The cytotoxicity of Asn-Tar/SeNPs was evaluated against the human breast cancer cell line MDA-MB-231. Cells were cultured in high-glucose DMEM supplemented with 10% fetal bovine serum (FBS; Gibco, USA) and 1% penicillin-streptomycin under 5% CO_2 and 95% humidity at 37 °C for 24 hours. Cells were treated with varying concentrations of the nanocomposite (31.25–1000 µg/mL) and incubated for 48 hours. Cytotoxicity was assessed using the MTT assay by adding 10 µL of MTT solution per well, followed by a 4-hour incubation. Subsequently, 100 µL of dimethyl sulfoxide (DMSO; Sigma-Aldrich, USA) was added to dissolve formazan crystals, and absorbance was measured at 595 nm using an ELISA reader. The half maximal inhibitory concentration (IC_{50}) was calculated accordingly.

Statistical Analysis

All quantitative experiments were performed in three independent replicates (n=3). Data are presented as mean±SD. Statistical analysis and graph plotting were performed using GraphPad Prism software (version 9.0 for Windows, GraphPad Software, San Diego, CA, USA).

The normality of data distribution was assessed using the Shapiro-Wilk test. For comparisons between two independent groups (e.g., cytotoxicity of nanocomposite on cancer cells vs. normal cells, inhibition zones of nanocomposite vs. antibiotic at a specific concentration), an unpaired two-tailed Student's *t* test was employed. For comparisons among more than two groups (e.g., antioxidant activity across different concentrations, bacterial growth inhibition at a fixed nanocomposite concentration across different bacterial strains), one-way analysis of variance (ANOVA) was used, followed by Tukey's *post hoc* test for multiple comparisons.

The half-maximal inhibitory concentration (IC_{50}) values for cytotoxicity and antioxidant activity were calculated by fitting the dose-response data to a non-linear regression (log(inhibitor) vs. response Variable slope) model in GraphPad Prism. The minimum inhibitory concentration (MIC) was determined as the lowest concentration that completely inhibited visible bacterial growth in the broth microdilution assay. A P value of less than 0.05 ($P<0.05$) was considered statistically significant for all tests.

Results

UV-Visible Spectrophotometry

The UV-Vis spectrum of the Asn-Tar/SeNPs nanocomposite, compared to Asn-Tar without nanoparticles, showed a distinct absorption band at 237 nm, indicating the surface plasmon resonance of SeNPs. The width of this peak indicates the particle size distribution in the nanocomposite. This finding confirms the formation and stability of SeNPs and is consistent with previous reports (figure 1).

Scanning Electron Microscope (SEM) Analysis

SEM analysis was used to evaluate the shape and size of the nanocomposite containing SeNPs. The nanocomposites were in the size range of 10–130 nm. As shown in figure 2, the Asn-Tar conjugated SeNPs were mostly spherical and appeared aggregated or clumped in some areas.

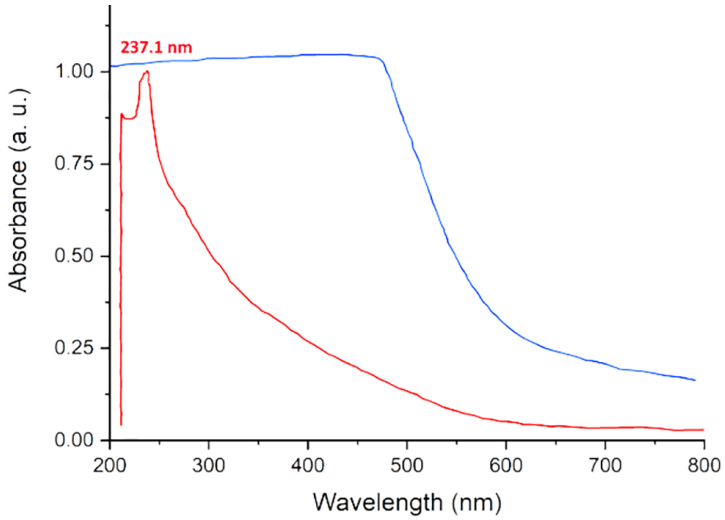

Figure 1: UV–visible (UV–Vis) absorption spectra of the Asn–Tar nanocomposite (blue) and the selenium-loaded Asn–Tar/selenium nanoparticles (SeNPs) nanocomposite (red) are shown.

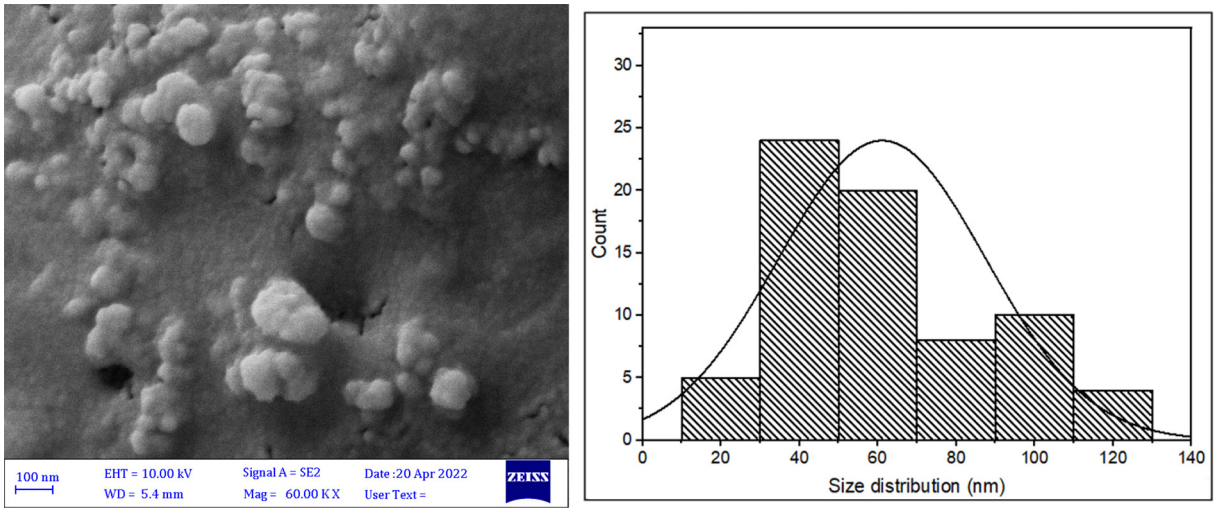

Figure 2: The figure shows the Scanning electron microscopy (SEM) image and corresponding diagram of selenium nanoparticles (SeNPs) loaded in the Asn–Tar/SeNPs nanocomposite.

Transmission Electron Microscope (TEM) Analysis and Energy-dispersive X-ray Spectroscopy (EDS)

To more accurately examine the size and structure of the nanoparticles, TEM imaging of the nanocomposite was performed. SeNPs within the Asn-Tar nanocomposites were observed to be mostly spherical and were irregular in some areas. The particle size was reported to be less than 200 nm. EDS analysis also confirmed the presence and abundance of the main elements in the nanocomposite composition (figure 3).

FTIR Analysis

FTIR analysis of the Asn-Tar/SeNPs nanocomposite revealed key functional group vibrations. A peak at 3430.3 cm^{-1} corresponds to the O–H stretching of tartaric acid's carboxyl groups, while the peak at 3316.4 cm^{-1} indicates the asymmetric stretching of the amino group in asparagine. Peaks at 3221.5 and 3025.3 cm^{-1} are attributed to CH and CH_2 stretching in tartaric acid's carbon skeleton. The strong peak at 1683.5 cm^{-1} reflects carbonyl stretching involved in tartaric acid–asparagine interactions. Symmetric stretching of deprotonated carboxyl groups appears at 1139.2 and 1088.6 cm^{-1}, and shear vibrations of tartaric acid's carboxyl appear at 835.4 cm^{-1}. Upon SeNPs incorporation, new peaks at 2924.0 and 2860.7 cm^{-1} indicate aliphatic CH and CH_2 groups on the nanoparticle surface, suggesting hydrophobic interactions. Signals at 1645.5 and 1740.8 cm^{-1} denote strong interactions between SeNPs and carbonyl and amine groups of the ligands. Additionally, peaks between 500–700 cm^{-1} confirm hydrostatic interactions between SeNPs and capping groups, including hydrated hydroxyls (figure 4).

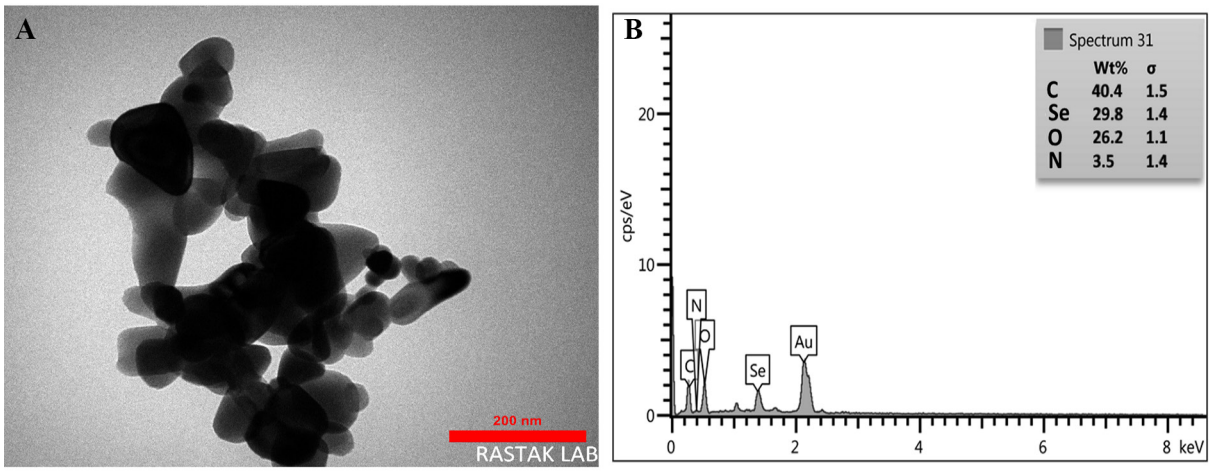

Figure 3: Morphological and elemental analysis of the Asn-Tar/Senps: (A) The figure shows the Transmission electron microscopy (TEM) image and (B) energy-dispersive X-ray spectroscopy (EDS) analysis diagram of the synthesized nanocomposite.

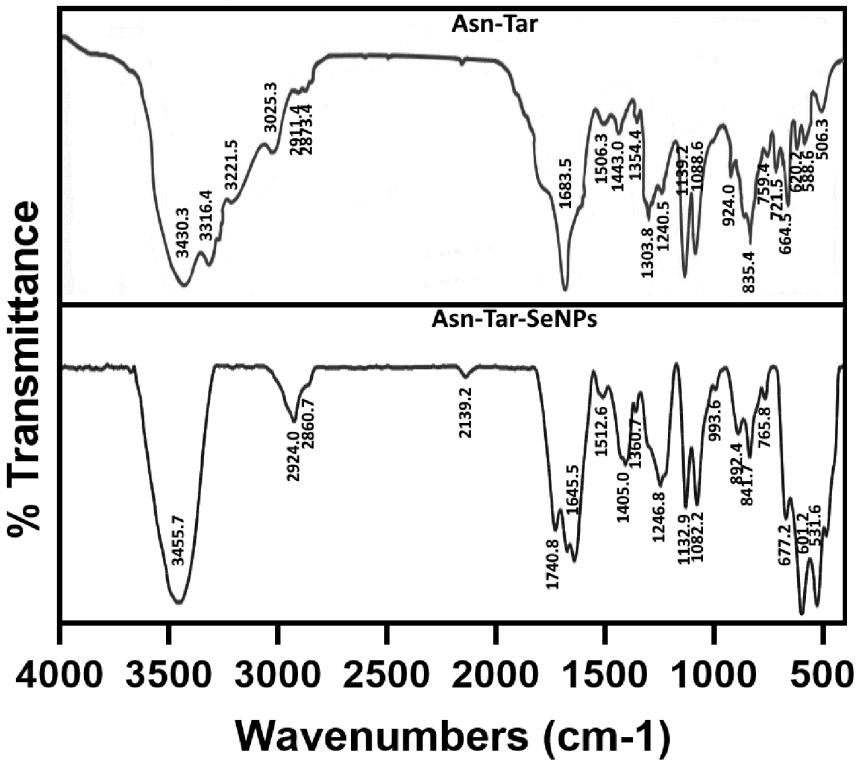

Figure 4: The figure shows the Fourier-transform infrared (FTIR) spectra of the Asn–Tar and Asn–Tar–SeNPs nanocomposites.

Size Distribution Analysis

Nanocomposite stability was assessed by measuring particle size and polydispersity index (PDI) in the aqueous phase. The SeNP-free nanocomposite had an average size of 60.67 nm, which increased to 460.8 nm after SeNP loading. Despite the size increase, the lower PDI indicated a more uniform size distribution in the selenium-containing nanocomposite (figure 5).

Nanoparticle Surface Charge Analysis (Zeta Potential)

Zeta potential measurements of Asn-Tar/SeNPs in solution showed a shift from +2.61±0.21 mV (without SeNPs) to −9.37±0.44 mV (with SeNPs) (n=3), indicating increased surface stability. These results are consistent with the moderate polydispersity index observed in dynamic light scattering (DLS) and the minor nanoparticle aggregation observed in microscopy (figure 6).

X-ray Crystallography (XRD) Analysis

XRD analysis revealed distinct sharp peaks at 2θ angles of 17.4°, 20.6°, 23.9°, 29.2°, 33.6°, and 38.5° for the Asn-Tar nanocomposite, indicating its crystalline structure. These peaks likely reflect crystalline organic compounds and interactions between asparagine and tartaric acid. In contrast,

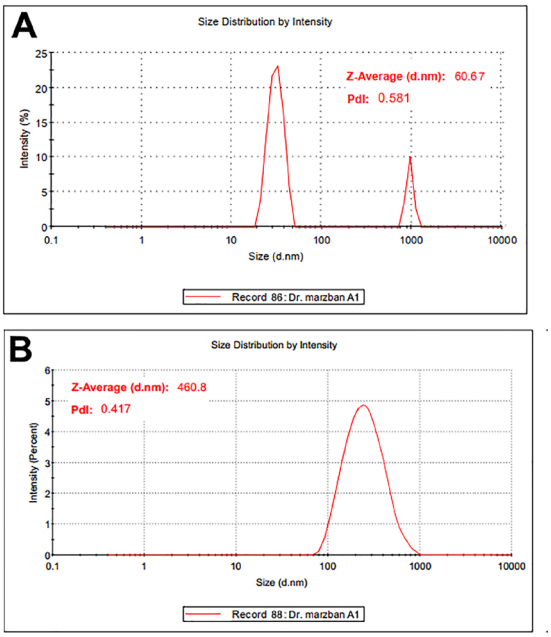

Figure 5: The size distribution of nanoparticles in the aqueous phase, as determined by Dynamic light scattering (DLS), is shown for (A) the Asn-Tar nanocomposite and (B) the Asn-Tar/SeNPs nanocomposite.

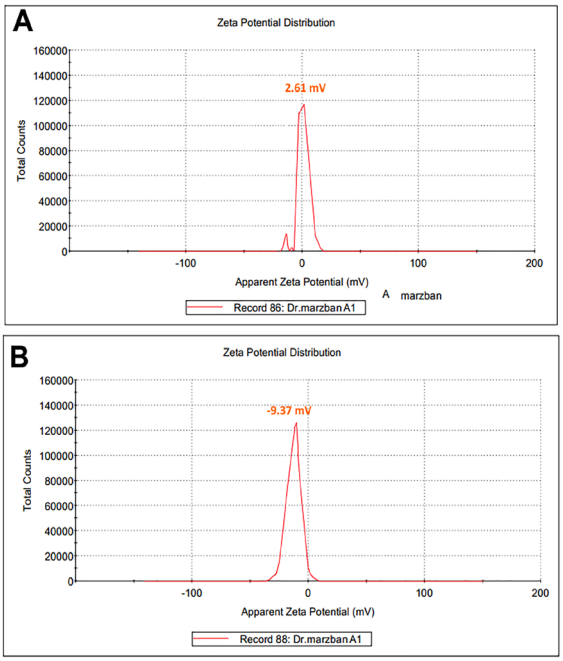

Figure 6: The zeta potential of the Asn-Tar nanocomposite is shown both with and without SeNPs.

the Asn-Tar/SeNPs nanocomposite exhibited broader, less intense peaks, particularly between 20° and 35°, indicating reduced crystallinity and a predominantly amorphous structure due to SeNP loading (figure 7).

Antimicrobial Activity Evaluation Based on MIC and MBC

Microdilution assays determined the MIC and MBC of the selenium nanocomposite against four bacterial strains. The nanocomposite effectively inhibited all tested bacteria, showing greater efficacy against Gram-positive strains. MIC and MBC values (mg/mL) were: *S. saprophyticus* (0.071, 0.065), *B. cereus* (0.069, 0.061), *K. pneumoniae* (0.054, 0.046), and *P. aeruginosa* (0.035, 0.047), with *S. saprophyticus* being the most sensitive. Optical density measurements confirmed dose-dependent bacterial growth inhibition, with reduced nanocomposite concentration correlating with increased bacterial growth (table 1).

Evaluation of Antimicrobial Activity Based on the Well Diffusion

The antimicrobial efficacy of Asn-Tar/SeNPs nanocomposite was evaluated against two Gram-negative (*K. pneumoniae*, *P. aeruginosa*) and two Gram-positive (*B. cereus*, *S. saprophyticus*) bacteria using the well diffusion method. Results demonstrated broad-spectrum activity, with the nanocomposite

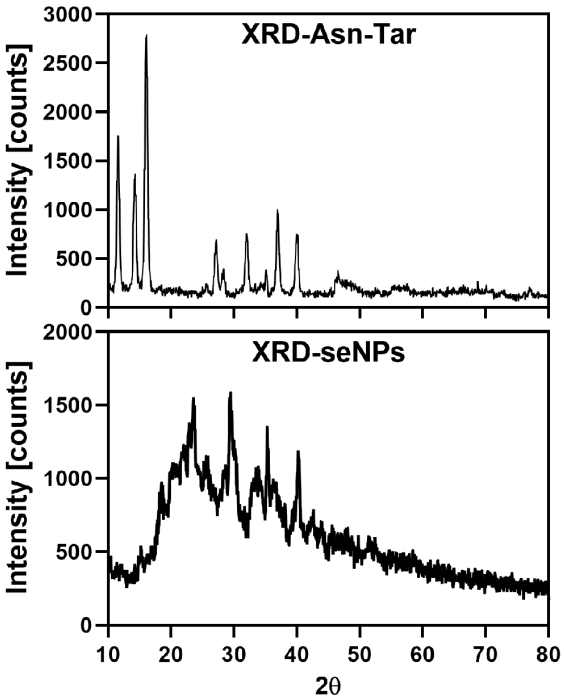

Figure 7: The X-ray diffraction (XRD) patterns for the nanocomposite without selenium and the nanocomposite containing SeNPs are visible in the image.

effectively inhibiting all tested strains at concentrations of 2.5, 5, 10, and 20 mg/mL (figure 8). Inhibition zones increased with concentration and were generally larger than those produced by the reference antibiotic chloramphenicol (10 mg/mL). At 20 mg/mL, the mean inhibition zone for *S. saprophyticus* was 36.9±1.2 mm (n=3,

P=0.0026) and for *B. cereus* was 35.84±1.1 mm (n=3, P=0.0032), which were significantly larger than those for chloramphenicol 26.18±0.8 mm (n=3, P=0.548). Among Gram-negative strains, *K. pneumoniae* showed the highest sensitivity, while *P. aeruginosa* was less affected. These findings are supported by MIC and MBC data (table 2).

Table 1: Results of antimicrobial activity evaluation based on middle inhibitory concentration (MIC) and Middle East Broadcasting Center (MBC) using microdilution method

Microorganism	Serial dilutions of Asn-Tar/SeNPs nanocomposite (mg/mL)								
	20	10	5	2.5	1.25	0.62	0.31	0.15	0.07
	Light absorption rate of bacterial activity in TCC reduction								
Bacillus cereus	0.012	0.014	0.022	0.032	0.057	0.061 [MBC]	0.069 [MIC]	0.28	0.86
Staphyococcus saprophyticus	0.010	0.013	0.024	0.036	0.043	0.049	0.056	0.065 [MBC]	0.071 [MIC]
Klebsilla pneumoniae	0.013	0.012	0.031	0.037	0.046 [MBC]	0.054 [MIC]	0.34	0.88	1.07
Pseudomonas aeruginosa	0.012	0.013	0.026	0.035 [MIC]	0.047 [MBC]	0.26	0.38	0.85	1.12

Table 2: Results of antimicrobial activity evaluation based on MIC and MBC using the microdilution method

Bacteria	Bacteria					
	Asn-Tar/SeNPs nanocomposite concentration (mg/mL)					Chloramphenicol (mg/mL)
	2.5	10	2.5	10	2.5	10
Klebsiella pneumoniae	13.59±0.1	31.4	13.59±0.1	31.4	13.59±0.1	31.4
Pseudomonas aeruginosa	15.17±0.62	28.13	15.17±0.62	28.13	15.17±0.62	28.13
Bacillus cereus	8.15±1.13	20.53	8.15±1.13	20.53	8.15±1.13	20.53
Staphylococcus saprophyticus	18.14±0.69	26.18	18.14±0.69	26.18	18.14±0.69	26.18

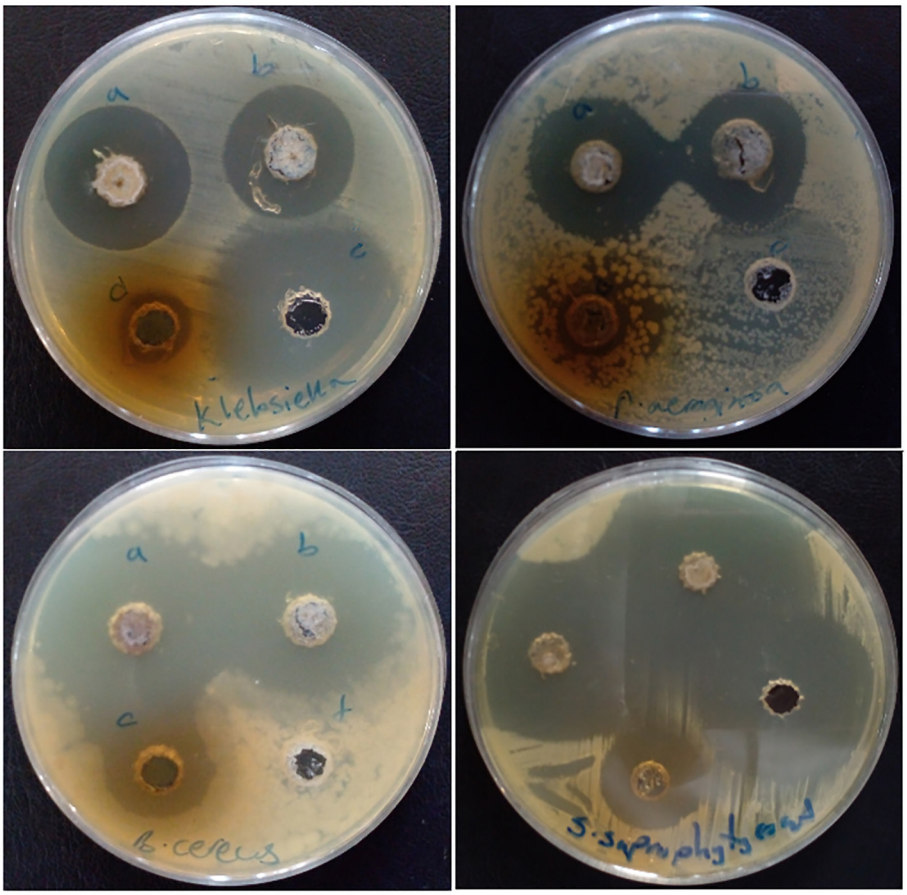

Figure 8: Culture plates of the tested bacteria using the well diffusion method are shown. The concentrations tested, from a to d, correspond to 20, 10, 5, and 2.5 mg/mL, respectively.

Antioxidant Activity (DPPH Scavenging Capacity)

The antioxidant capacity of Asn-Tar/SeNP nanocomposite was assessed using the DPPH radical scavenging assay and compared to ascorbic acid (AA) and butylated hydroxytoluene (BHT). The nanocomposite exhibited dose-dependent DPPH scavenging activity. The IC_{50} value for the Asn-Tar/SeNP nanocomposite was 22.73±1.55 µg/mL (n=3) for DPPH scavenging, compared to ascorbic acid (11.87±0.98 µg/mL, n=3, P=0.0081) and BHT (5.89±0.64 µg/mL, n=3, P=0.0015), with significant differences (P=0.014). Nonetheless, the results confirm that the nanocomposite possesses measurable antioxidant activity (figure 9).

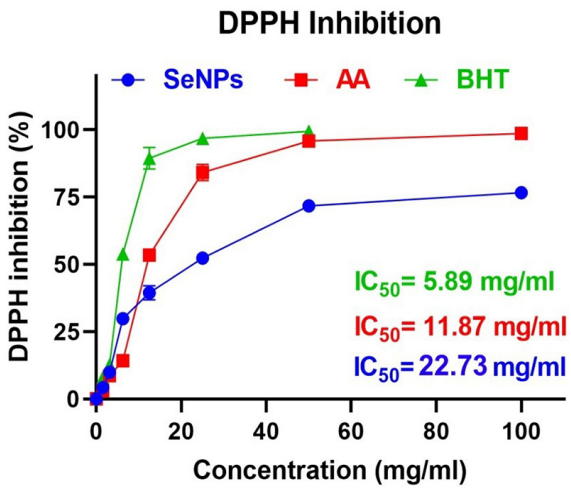

Figure 9: The antioxidant activity of the Asn-Tar/SeNPs nanocomposite compared to ascorbic acid (AA) and butylated hydroxytoluene (BHT), as measured by the 2,2-diphenyl-1-picrylhydrazyl (DPPH) scavenging assay, is shown in the figure.

Antioxidant Activity (Inhibition Test H2O2)

The antioxidant activity of the selenium nanocomposite was further evaluated by its ability to scavenge hydrogen peroxide. The IC_{50} for hydrogen peroxide inhibition was 42.14±2.08 µg/mL (n=3), which was significantly higher than that of ascorbic acid (11.15±0.63 µg/mL, n=3; P=0.0008), indicating lower antioxidant efficacy (figure 10).

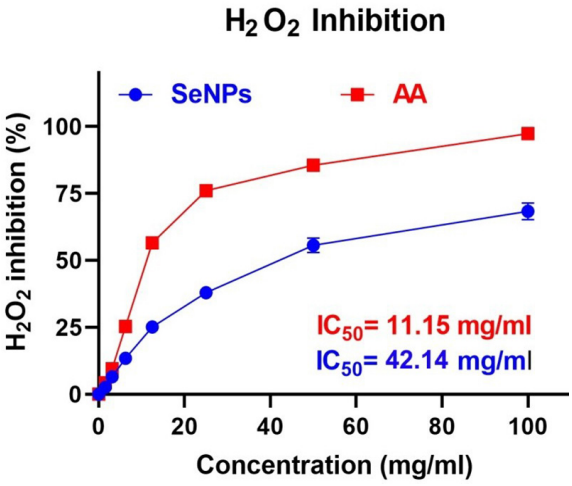

Figure 10: This image shows the hydrogen peroxide inhibition activity of the Asn-Tar/SeNPs nanocomposite.

Cytotoxicity Assay

The cytotoxicity of the Asn-Tar/SeNPs nanocomposite was evaluated against MDA-MB-231 breast cancer cells and normal fibroblast cells. The IC_{50} value for MDA-MB-231 cells was 3.47±0.28 µg/mL (n=3), while for normal fibroblast cells it was 5.91±0.34 µg/mL (n=3). The difference between the two IC_{50} values was statistically significant (P=0.0051), indicating selective cytotoxicity toward the cancer cells. The calculated selectivity index (SI=IC_{50}[normal]/IC_{50}[cancer]) was approximately 1.7, further confirming the higher toxicity of the nanocomposite against cancer cells (figure 11).

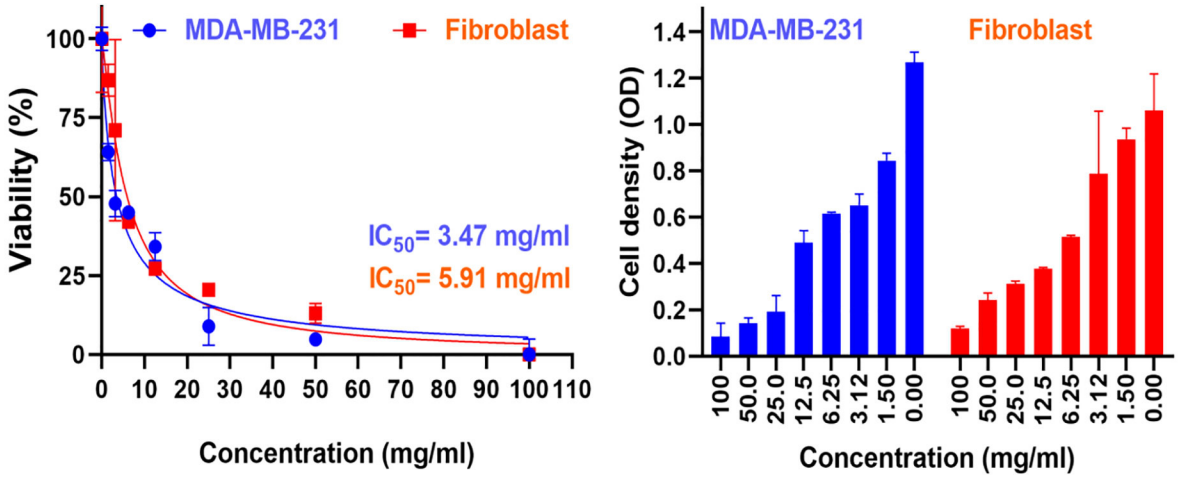

Figure 11: Cytotoxicity of Asn-Tar/SeNPs nanocomposite on MDA-MB-231 cancer cells and normal fibroblasts, with IC50 values shown in the image.

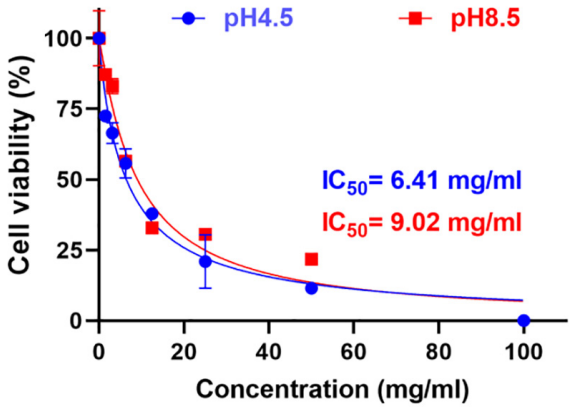

Figure 12: The anticancer activity of Asn-Tar/SeNPs nanocomposite under different acidic (pH 4.5) and alkaline (pH 8.5) conditions against the MDA-MB-231 cancer cell line is clearly shown in the image.

Effect of pH on Cytotoxicity

The nanocomposite retained approximately 50% of its anticancer activity at acidic pH (4.5) and 25% at basic pH (8.5), indicating pH-dependent efficacy. These results highlight the importance of physiological pH in optimizing nanocomposite-based drug delivery systems (figure 12).

Discussion

In the present study, Asn-Tar/SeNPs nanocomposites were successfully synthesized and exhibited significant antimicrobial, antioxidant, and cytotoxic activities on MDA-MB-231 breast cancer cells.

The nanoparticles used in this study were synthesized using the co-precipitation method. Subsequently, the SeNPs coated with L-asparagine and tartaric acid were characterized using techniques such as TEM, XRD, SEM, UV-visible absorption spectroscopy, FTIR spectroscopy, DLS measurement, and zeta potential. The analysis of the UV-visible absorption spectrum showed that the size of SeNPs loaded in the Asn-Tar nanocomposite was in the range of 20–240 nm, which is consistent with the results of Bartosiak and others, who reported the size of SeNPs in the range of 20–240 nm.[14]

SEM analysis showed that the SeNPs loaded in the Asn-Tar nanocomposite had an almost spherical morphology and were aggregated in some areas, and also showed a size distribution of approximately 10 to 130 nm. TEM results provided more complete information on the particle size and the effect of the nanocomposite intercalation with SeNPs. TEM determined the particle size in the range of below 200 nm and the structure of SeNPs inside the Asn-Tar nanocomposite as almost spherical, and in some irregular areas. In addition, EDS analysis, which determines the percentage of elements constituting the nanocomposite, showed that the nanocomposite had a high efficiency in loading SeNPs. The results of SEM and TEM analysis in our study, which determined the size of SeNPs to be below 200 nm and with spherical morphology, are consistent with many studies, including Prasad's study in 2013 and Ramamurthy's study in 2013, as well as Dhanraj's study in 2021.[15-17]

FTIR analysis confirmed the successful interaction between SeNPs and tartaric acid and asparagine. This analysis showed that strong cross-linking was formed between SeNPs at the sites where the carbonyl and amine groups of tartaric acid and asparagine were present. This modified the surface of SeNPs, changed the surface of SeNPs, and increased their stability. DLS results showed that the selenium-containing nanocomposite was larger in size, but more uniform and stable in terms of homogeneity (PDI) in the aqueous phase than the nanocomposite. The significant increase in the size of the nanocomposite by DLS from 60.67 nm to 460.8 nm after SeNP loading indicates significant structural changes after functionalization. This size increase may be attributed to the formation of a thick organic coating layer consisting of tartaric acid and L-asparagine. These modifications could facilitate effective interactions with cell membranes or enhance the controlled release of selenium ions, thereby contributing to cytotoxic and antimicrobial effects. Additionally, the surface charge of the Asn-Tar/SeNP nanocomposites in the aqueous phase was determined by determining the zeta potential index. It was found that with the introduction of SeNPs into the nanocomposite structure, its net charge became negative, while the nanocomposite without SeNPs had a positive charge. According to studies, nanoparticles with a negative charge of less than -30 mV and more than +30 mV have been found to have the highest stability.[18, 19] These results were consistent with the results obtained from DLS.

The XRD peaks of the selenium-free nanocomposite have distinct peaks and are more regular in the form of a crystalline phase. However, the Asn-Tar/SeNPs nanocomposite has very irregular peaks, indicating the amorphous nature of the selenium-containing nanocomposite.

In this study, SeNPs loaded in the Asn-Tar nanocomposite showed good antimicrobial activity against both Gram-positive and Gram-negative bacteria. This was particularly evident in their ability to inhibit the growth and

proliferation of antibiotic-resistant bacteria. Importantly, SeNPs alone showed less antimicrobial activity than the nanocomposite. Prior research has established the antibacterial effectiveness of SeNPs-based nanoparticles against both Gram-positive and Gram-negative bacterial strains; for instance, Hernández-Díaz and others noted a more pronounced inhibitory effect of SeNPs on Gram-negative bacteria. Their results indicate that SeNPs provide enhanced antimicrobial activity compared to the use of marigold extracts or sodium selenite (Na2SeO3) alone.[20] Additionally, in 2021, Zhang and colleagues illustrated the antibacterial properties of Gram-positive and Gram-negative SeNPs.[21] Notably, in line with our results, a study by Bu and colleagues in 2024 showed that surface modification of SeNPs leads to enhanced antibacterial properties of SeNPs without modification or alteration of the surface chemistry.[22]

We demonstrated that Asn-Tar/SeNP nanocomposite has antioxidant properties by investigating the DPPH scavenging capacity and hydrogen peroxide (H2O2) scavenging activity. The results of Lakshmi's study in 2025 also indicate the high capacity of SeNPs in scavenging H2O2 and DPPH.[23]

The significant antioxidant activity of the Asn-Tar/SeNPs nanocomposite suggests a plausible hypothesis for its selective cytotoxicity against cancer cells. Cancer cells typically exhibit elevated levels of reactive oxygen species (ROS) and are more susceptible to oxidative stress-induced apoptosis. We hypothesize that the ROS-scavenging ability of the nanocomposite could perturb the redox homeostasis of MDA-MB-231 cells, potentially triggering apoptotic pathways or inhibiting proliferation.[24] Furthermore, such antioxidant activity might concurrently offer a protective effect to normal cells against oxidative damage, thereby possibly enhancing the observed selective cytotoxicity. This proposed mechanism aligns with the literature that suggests modulation of oxidative stress is a crucial aspect of the anticancer mechanisms of selenium nanoparticles.[4]

We synthesized Asn-Tar/SeNPs nanocomposite with the aim of reducing toxicity and increasing stability of selenium nanoparticles. Tartaric acid and L-asparagine increased the biocompatibility and stability of selenium nanoparticles, as well as maintained their antibacterial and antioxidant properties. We confirmed these properties using agar diffusion, MIC, and MBC methods against Gram-positive and Gram-negative bacteria. It is worth noting that SeNPs coated with tartaric acid and L-asparagine showed acceptable antimicrobial effects and showed inhibitory effects against antibiotic-resistant bacteria such as *S. saprophyticus*, *B. cereus*, *K. pneumoniae,* and *P. aeruginosa*. Previous studies have shown that the reduced efficacy of SeNPs against bacteria and increased toxicity in cells is due to the surface chemistry of SeNPs, and their surface modification can lead to reduced toxicity and higher inhibition against bacteria.[22, 25, 26] Our findings also confirm the results of the studies, which show that surface modification of SeNPs with tartaric acid and L-asparagine can have a higher affinity for the hydrophobic surface of Gram-negative bacteria, thereby facilitating the penetration stability of nanoparticles.

Similarly, the MIC of our nanocomposite against *S. saprophyticus* (0.071 mg/mL) was lower than that reported for folic acid functionalized SeNPs (0.1 mg/mL), indicating higher antibacterial activity against resistant strains.[6]

In the present study, the cytotoxicity of selenium nanocomposites was evaluated on the MDA-MB-231 cancer cell line. The findings showed that the selenium nanocomposite had significant cytotoxicity against MDA-MB-231 cells (IC_{50}=3.47±0.28 µg/mL). In other studies, uncoated SeNPs had an IC_{50}≈34 µg/mL, indicating the enhanced efficacy resulting from functionalization of the SeNP surface.[4, 15]

We also investigated the effect of pH changes on the anticancer activity of SeNPs loaded in Asn-Tar nanocomposite. The results showed that the nanocomposite maintained its anticancer activity against the MDA-MB-231 cancer cell line at about 50% at acidic pH (PH 4.5) and about 25% at basic pH (PH 8.5). Therefore, the high stability and maintenance of efficacy of the nanocomposites synthesized in this study under acidic and basic conditions can be clearly observed. Many studies have been conducted in line with our results and have shown the anticancer properties of SeNPs on many cancer cell lines, and we will mention some of these studies below. İpek and colleagues in 2024 demonstrated the anticancer potential of SeNPs on glioblastoma cells (U373), osteosarcoma cells (U2OS), and healthy retinal pigment epithelial cell lines (RPE-1) using the MTT assay.[27] Gulbay also conducted a study in 2023 to investigate the potential anticancer properties of thymoquinone (TQ)-encapsulated SeNPs (TQ-SeNPs) in HEC1B endometrial cancer cells. The results of his study showed that these nanoparticles have a high antiproliferative effect on endometrial cancer cells.[28] In addition, in a recent study conducted by Mahmood and

colleagues (2025), it was shown that apoptosis can be induced in the human lung cancer cell line A549 by exposure to SeNPs and selenium chitosan nanoparticles.[29]

However, this study, similar to all other studies, has limitations. All analyses were performed *in vitro,* and only one cancer cell line was used to assess cytotoxicity. Furthermore, cell signaling pathways were not investigated. Future studies should address these limitations with *in vivo* experiments and larger studies.

This study has some limitations that should be acknowledged. First, experimental controls using uncoated (bare) selenium nanoparticles (SeNPs) and the ligand mixture (L-asparagine and tartaric acid) alone were not included. Consequently, while our results demonstrate the potent biological activity of the Asn-Tar/SeNPs nanocomposite, we cannot definitively dissect the individual contribution of the SeNP core versus the organic coating to the observed effects, nor can we make direct quantitative comparisons about the enhancement conferred by functionalization. Future studies incorporating these controls would provide a more mechanistic understanding of the structure-activity relationship. Second, all evaluations were performed *in vitro*; thus, *in vivo* efficacy and safety remain to be investigated.

Conclusion

The findings of the present study demonstrate the potential of Asn-Tar/SeNPs nanocomposite in biomedicine. This nanocomposite exhibited significant antimicrobial activity, especially against antibiotic-resistant bacterial strains. It also exhibited significant antioxidant properties and effectively inhibited the growth of MDA-MB-231 cancer cells even with high pH changes. Since antibiotic-resistant bacteria are increasing day by day, cancer is also increasing, and current antibiotics and conventional drugs have harmful side effects, we propose to attach specific ligands, such as antibodies or oligonucleotides, to this nanocomposite. This can enhance their therapeutic effects while reducing side effects.

Acknowledgment

This study is derived from the Master's thesis of the co-first author, Khadije Salari Nejad, entitled "Synthesis and evaluation of selenium nanoparticles functionalized with L-asparagine and tartaric acid and investigation of their anticancer and antibacterial effects", submitted to the Department of Medical Biotechnology, Lorestan University of Medical Sciences. The research did not receive any specific grant from funding agencies.

The authors would like to express their gratitude to the clinical research development unit of Imam Khomeini Hospital, Urmia University of Medical Sciences, for English editing. The authors would like to thank Khorramabad University of Medical Sciences for providing technical support and facilities during this research. The authors also acknowledge the contributions of colleagues who provided valuable insights during the design and analysis of the experiment.

All data interpretation, scientific conclusions, and final approval of the content were performed by the authors.

Authors' Contribution

All authors contributed to study conception and design, supervision, writing, and critical revision of the manuscript. All authors have read and approved the final manuscript and agree to be accountable for all aspects of the work in ensuring that questions related to the accuracy or integrity of any part of the work are appropriately investigated and resolved.

Declaration of AI

The latest version of Quillbot's artificial intelligence (AI) was used to improve the clarity, grammar, and style of certain sentences originally written by the authors. The authors are fully responsible for the content and integrity of the manuscript.

Conflict of Interest: None declared.

References

1 Chehelgerdi M, Chehelgerdi M, Allela OQB, Pecho RDC, Jayasankar N, Rao DP, et al. Progressing nanotechnology to improve targeted cancer treatment: overcoming hurdles in its clinical implementation. Mol Cancer. 2023;22:169. doi: 10.1186/s12943-023-01865-0. PubMed PMID: 37814270; PubMed Central PMCID: PMC10561438.

2 Sengar A. The Role of Nanotechnology in Revolutionizing Cancer Treatment. Preprints. 2025. doi: 10.20944/preprints202503.0713.v1.

3 Eltaib L. Polymeric Nanoparticles in Targeted Drug Delivery: Unveiling the Impact of Polymer Characterization and Fabrica-tion. Polymers (Basel). 2025;17. doi: 10.3390/

polym17070833. PubMed PMID: 40219222; PubMed Central PMCID: PMC11991310.
4 Anjum S, Hashim M, Imran M, Babur S, Adnan S, Hano C, et al. Selenium Nanoparticles in Cancer Therapy: Unveiling Cytotoxic Mechanisms and Therapeutic Potential. Cancer Rep (Hoboken). 2025;8:e70210. doi: 10.1002/cnr2.70210. PubMed PMID: 40452566; PubMed Central PMCID: PMC12127775.
5 Waqar MA. A comprehensive review on recent advancements in drug delivery via selenium nanoparticles. J Drug Target. 2025;33:157-70. doi: 10.1080/1061186X.2024.2412142. PubMed PMID: 39392210.
6 Chen W, Cheng H, Xia W. Progress in the Surface Functionalization of Selenium Nanoparticles and Their Potential Application in Cancer Therapy. Antioxidants (Basel). 2022;11. doi: 10.3390/antiox11101965. PubMed PMID: 36290687; PubMed Central PMCID: PMC9598587.
7 Bisht N, Phalswal P, Khanna PK. Selenium nanoparticles: a review on synthesis and biomedical applications. Mater Adv. 2022;3:1415-31. doi: 10.1039/D1MA00639H.
8 Handy DE, Joseph J, Loscalzo J. Selenium, a Micronutrient That Modulates Cardiovascular Health via Redox Enzymology. Nutrients. 2021;13. doi: 10.3390/nu13093238. PubMed PMID: 34579115; PubMed Central PMCID: PMC8471878.
9 Candido AC, Azevedo FM, Machamba AAL, Pinto CA, Lopes SO, de Souza Macedo M, et al. Implications of iodine deficiency by gestational trimester: a systematic review. Arch Endocrinol Metab. 2021;64:507-13. doi: 10.20945/2359-3997000000289. PubMed PMID: 34033289; PubMed Central PMCID: PMC10118970.
10 Raja P, Rajkumar P, Jegatheesan P, Amalraj AS, Rajah AJL. Investigation of structural, optical and photoluminescence properties of non-essential amino acid capped zinc sulfide nanoparticles for optoelectronic applications. J Indian Chem Soc. 2023;100:100855. doi: 10.1016/j.jics.2022.100855.
11 Li M, Su J, Yang H, Feng L, Wang M, Xu G, et al. Grape tartaric acid: chemistry, function, metabolism, and regulation. Horticulturae. 2023;9:1173. doi: 10.3390/horticulturae9111173.
12 Jantwal A, Durgapal S, Upadhyay J, Joshi T, Kumar A. Tartaric acid. In: Antioxidants effects in health. Amsterdam: Elsevier; 2022. p. 485-92. doi: 10.1016/B978-0-12-819096-8.00013-6.
13 Weinstein MP, Lewis JS, 2nd. The Clinical and Laboratory Standards Institute Subcommittee on Antimicrobial Susceptibility Testing: Background, Organization, Functions, and Processes. J Clin Microbiol. 2020;58. doi: 10.1128/JCM.01864-19. PubMed PMID: 31915289; PubMed Central PMCID: PMC7041576.
14 Bartosiak M, Giersz J, Jankowski K. Analytical monitoring of selenium nanoparticles green synthesis using photochemical vapor generation coupled with MIP-OES and UV-Vis spectrophotometry. Microchem J. 2019;145:1169-75. doi: 10.1016/j.microc.2018.12.024.
15 Prasad KS, Patel H, Patel T, Patel K, Selvaraj K. Biosynthesis of Se nanoparticles and its effect on UV-induced DNA damage. Colloids Surf B Biointerfaces. 2013;103:261-6. doi: 10.1016/j.colsurfb.2012.10.029. PubMed PMID: 23201746.
16 Ramamurthy C, Sampath KS, Arunkumar P, Kumar MS, Sujatha V, Premkumar K, et al. Green synthesis and characterization of selenium nanoparticles and its augmented cytotoxicity with doxorubicin on cancer cells. Bioprocess Biosyst Eng. 2013;36:1131-9. doi: 10.1007/s00449-012-0867-1. PubMed PMID: 23446776.
17 Dhanraj G, Rajeshkumar S. Anticariogenic effect of selenium nanoparticles synthesized using Brassica oleracea. J Nanomater. 2021;2021:8115585. doi: 10.1155/2021/8115585.
18 Alallam B, Oo MK, Nasir MHM, Taher M. Influence of nanoparticles surface coating on physico-chemical properties for CRISPR gene delivery. J Drug Deliv Sci Technol. 2021;66:102910. doi: 10.1016/j.jddst.2021.102910.
19 Gauggel S, Derreza-Greeven C, Wimmer J, Wingfield M, van der Burg B, Dietrich DR. Characterization of biologically available wood combustion particles in cell culture medium. ALTEX. 2012;29:183-200. doi: 10.14573/altex.2012.2.183. PubMed PMID: 22562490.
20 Hernandez-Diaz JA, Garza-Garcia JJ, Leon-Morales JM, Zamudio-Ojeda A, Arratia-Quijada J, Velazquez-Juarez G, et al. Antibacterial Activity of Biosynthesized Selenium Nanoparticles Using Extracts of Calendula officinalis against Potentially Clinical Bacterial Strains. Molecules. 2021;26. doi: 10.3390/molecules26195929. PubMed PMID: 34641478; PubMed Central PMCID: PMC8513099.
21 Zhang H, Li Z, Dai C, Wang P, Fan S, Yu B, et al. Antibacterial properties and

mechanism of selenium nanoparticles synthe-sized by Providencia sp. DCX. Environ Res. 2021;194:110630. doi: 10.1016/j.envres.2020.110630. PubMed PMID: 33345899.
22 Bu Q, Jiang D, Yu Y, Deng Y, Chen T, Xu L. Surface chemistry engineered selenium nanoparticles as bactericidal and immuno-modulating dual-functional agents for combating methicillin-resistant Staphylococcus aureus Infection. Drug Resist Updat. 2024;76:101102. doi: 10.1016/j.drup.2024.101102. PubMed PMID: 38936006.
23 Lakshmi T, Rajeshkumar S, Dinesh G. Green synthesis of selenium nanoparticles using Vaccinium subg. Oxycoccus for antioxidant, anti-inflammatory, and cytotoxic effect. Trop J Pharm Health Res. 2013;13:61-7. doi: 10.21522/TIJPH.2013.13.01.Art061.
24 Sabzevari AG, Sabahi H, Nikbakht M, Azizi M, Dianat-Moghadam H, Amoozgar Z. Exploring the Potential of Montmorillonite as an Antiproliferative Nanoagent against MDA-MB-231 and MCF-7 Human Breast Cancer Cells. Cells. 2024;13. doi: 10.3390/cells13020200. PubMed PMID: 38275825; PubMed Central PMCID: PMC10814472.
25 Pi J, Shen L, Yang E, Shen H, Huang D, Wang R, et al. Macrophage-Targeted Isoniazid-Selenium Nanoparticles Promote Antimicrobial Immunity and Synergize Bactericidal Destruction of Tuberculosis Bacilli. Angew Chem Int Ed Engl. 2020;59:3226-34. doi: 10.1002/anie.201912122. PubMed PMID: 31756258.
26 Hosnedlova B, Kepinska M, Skalickova S, Fernandez C, Ruttkay-Nedecky B, Malevu TD, et al. A Summary of New Findings on the Biological Effects of Selenium in Selected Animal Species-A Critical Review. Int J Mol Sci. 2017;18. doi: 10.3390/ijms18102209. PubMed PMID: 29065468; PubMed Central PMCID: PMC5666889.
27 İpek P, Baran A, Hatipoğlu A, Baran MF. Cytotoxic potential of selenium nanoparticles (SeNPs) derived from leaf extract of Mentha longifolia L. J Agric Environ Food Sci. 2024;8:169-75. doi: 10.31015/jaefs.2024.1.17.
28 Gulbay G, Secme M, Ilhan H. Exploring the Potential of Thymoquinone-Stabilized Selenium Nanoparticles: In HEC1B Endometrial Cancer Cells Revealing Enhanced Anticancer Efficacy. ACS Omega. 2023;8:39822-9. doi: 10.1021/acsomega.3c06028. PubMed PMID: 37901525; PubMed Central PMCID: PMC10601430.
29 Mahmood RI, Al-Taie A, Al-Rahim AM, Mohammed-Salih HS, Ibrahim HA, Albukhaty S, et al. Biogenic synthesized se-lenium nanoparticles combined chitosan nanoparticles controlled lung cancer growth via ROS generation and mito-chondrial damage pathway. Nanotechnol Rev. 2025;14:20250142. doi: 10.1515/ntrev-2025-0142.